

Climatology of Mesospheric Temperature Profiles Observed With the Consortium Rayleigh-Scatter Lidar at Logan, Utah

V.B. Wickwar¹, K.C. Beissner¹, T.D. Wilkerson¹, S.C. Collins¹, J.M. Maloney¹
J.W. Meriwether, Jr.², X. Gao²

¹Center for Atmospheric & Space Sciences, Utah State University
Logan, UT 84322-4405, USA. E-mail: wickwar@aeronomy.cass.usu.edu

²Dept. of Physics and Astronomy, Clemson University
Clemson, SC 29634-1911, USA. E-mail: john.meriwether@ces.clemson.edu

Abstract. From Aug. 1993 to Feb. 1996, regular Rayleigh-scatter observations of the stratosphere and mesosphere in the altitude range 40–95 km were made with the Consortium Lidar (CL) located at Utah State University. These observations are now being continued with the Atmospheric Lidar Observatory (ALO) at the same location. The site is located at mid latitude in the middle of the Rocky Mountains—41.75° N, 111.80° W. Atmospheric density profiles derived from the lidar returns are reduced to temperature profiles, with considerable care being taken to avoid possible systematic errors. In summer months, the Utah mesospheric temperatures, like those from elsewhere, show the least variability and the expected monotonic decrease of temperature with altitude. However, the Utah temperatures appear systematically lower than others. Between spring and fall, an important feature of the temperature climatology is a strong asymmetry, which appears to be larger than elsewhere. In winter, day-to-day temperature variability is greatest, but variability also exists on the scale of a week. Perhaps as a consequence, or perhaps for another reason, the Utah data show an enormous change from one January to the next. Are these differences in the climatology real? If so, can they be related to the mountainous location and the orographic generation of gravity waves? Can the temporal variations be related to planetary (Rossby) waves and the generation of gravity waves by the jet stream?

1. Description of the Rayleigh-Scatter Lidar System

The 532-nm beam originates from a Spectra Physics, seeded, 30 Hz, Nd:YAG laser. It exits the building toward the zenith, coaxial with a 44-cm receiving telescope. [For the CL, the laser was a GCR-6 operating at 24 W, giving a power-aperture product (PAP) of 3.6 W-m². For the ALO, the laser is a GCR-5 operating at 19 W, giving a PAP of 2.9 W-m². However, later this year ALO will switch to a much larger telescope, increasing the PAP to 88 W-m². These smaller values are comparable to those of several Rayleigh-scatter lidars around the world.] The field of view of the telescope is set to 1.0–1.5 mrad to comfortably encompass the laser beam's divergence of ≤ 0.5 mrad without picking up too much background light. The telescope output is directly coupled into the detector chamber. A chopper blocks the most intense backscatter from the lowest altitudes, and electronic gating protects the photomultiplier tube (PMT) the rest of the way up to the altitude of interest. The chopper is also the nominal 30-Hz source for firing the laser flash lamps. The PMT is cooled to extend the altitude range as high as possible. The PMT signal is amplified and sent to an EG&G multi-channel scaler. The data-acquisition trigger

comes from the Q-switch, thereby avoiding range errors that might be introduced by chopper fluctuations. Each channel is sampled every 250 ns (37.5 m) in 14,000 range bins (525 km) and integrated for 3,600 shots (2 minutes). We have found the large number of range bins very useful for detecting output problems arising from either high signal levels or the gating circuit. The data are displayed in real time and stored to disk.

2. Derivation of Rayleigh-Scatter Temperatures

The temperatures are derived for hydrostatic equilibrium of an ideal gas, with the downward integration beginning at the altitude where the signal is equivalent to 16 standard deviations. Originally, the initial temperature value was taken from the MSISE90 model [1]. But it led to such a large gradient in winter that it appeared to be too low a temperature. Now the initial value is derived from the Ft. Collins averages [2] with a superimposed time variation from MSISE90. In the integration, the sea-level value of g appropriate for USU is taken to be 9.80255 m/s^2 , and the mean molecular mass has been allowed to vary with altitude according to the MSISE90 model. At the higher altitudes, this means we take into account a changing average scattering cross section and, in the integration, a changing mass. To smooth the data prior to data reduction, we average it for 3 km in altitude and over varying intervals in time ranging from one hour to a whole night. We are also searching for the most meaningful way to make an all-night or an all-month average.

3. Low Mesospheric Summer Temperatures above Utah

In Fig. 1 we show the average temperature profile for June 1994. It is based on 6 nights of observations, each night having approximately 4 hours of data. For comparison, profiles are also shown from the MSISE90 model [1], the French lidar data from Haute Provence (44°N , 6°E) and Biscarrosse (44°N , 1°W) [3], and the SME satellite (40°N) [4]. Above 82 km, sodium lidar temperatures from Fort Collins (41°N , 105°W) [2] are also shown. Between 45 and 80 km, reasonable agreement exists among the four curves, particularly among the MSISE90, Utah lidar, and French lidars, giving us considerable confidence in our results. The agreement with

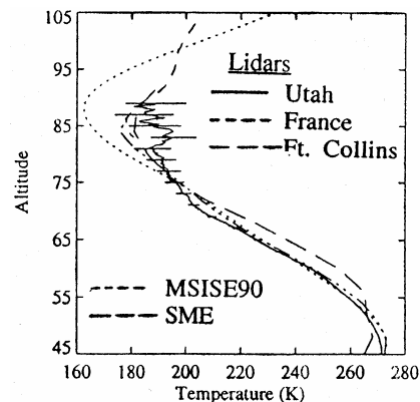


Fig. 1. June temperature profiles.

MSISE90 over much of the altitude range (below 77 km) is especially encouraging because its curve is based on different techniques, mostly on rocket data and satellite data. However, some differences do exist. In particular, near 70 km, the Utah temperatures are consistently about 7 K cooler than the others. In addition, above 77 km all the observations are higher than the MSISE90 temperatures and between 55 and almost 70 km all the observations are consistently 10 K cooler than the SME values.

4. Large Spring-Fall Mesospheric Asymmetry above Utah

The left part of Fig. 2 shows the observed annual variation of mesospheric temperatures between 45 and 85 km based on monthly averages derived from the first 20 months of operation. The right part shows the corresponding contours from the MSISE90 model. The highest temperature contour is for 270 K; the lowest for 180 K; each step is 10 K. Basically, the two sets of contours are similar, showing a cold

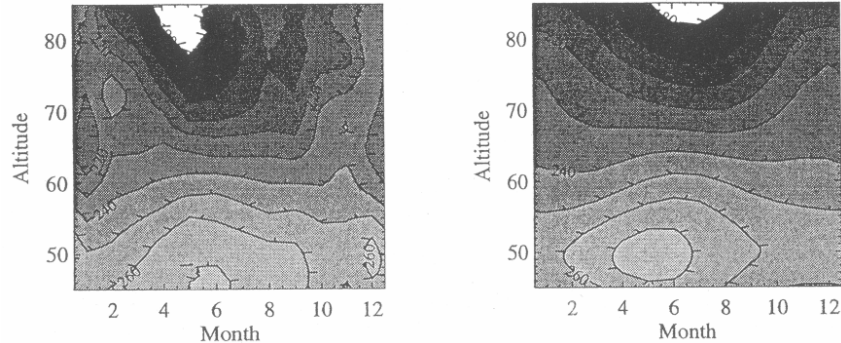


Fig. 2. Annual variation of mesospheric temperature—Utah data & MSISE90.

mesopause in summer, a warm mesopause in winter, and a warm stratopause in summer. Beyond that, the observations compared to the model show significant differences: the summer mesopause minimum occurs almost two months earlier; consistent with Fig. 1, the early-summer temperature gradient near 65–70 km is steeper; a winter minimum occurs in the mesospheric temperatures near 65 km; the upper mesosphere is warmer in the winter half of the year; and the summer stratopause occurs at a lower altitude. Having the coldest, upper mesospheric temperatures centered about early May leads to a major temperature asymmetry between spring and fall. That this asymmetry is real is supported by a very strong asymmetry in the OH winds from 87 km observed with a nearby Fabry-Perot interferometer.

5. Major Differences Between January 1994 and January 1995

In Fig. 3 we show the average temperature profiles for January 1994 and 1995. The feature that stands out most strongly in both profiles is the mesospheric inversion layer [5, 6, 7, 4, 8], a temperature increase with respect to MSISE90 of 10 to 50 K. In both cases, the altitude is significantly higher than that in statistical studies [6, 8]. Almost as obvious is a relative temperature minimum 10–20 km below the inversion-layer peak. The two features together give the

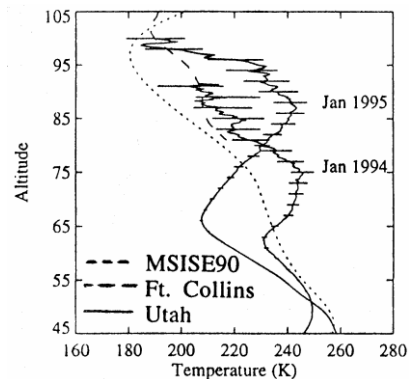


Fig. 3. January temperature profiles.

appearance of a wave with respect to the model profile. Another major feature, possibly a new one, is the large change in altitude and magnitude of the inversion layer from one year to the next. Within a given winter (not shown), the nightly profiles are similar for a week or so and then change abruptly to another pattern. This might account for the change in Fig. 3, or we may have to look elsewhere.

6. Conclusion—Lidar Working Group

In these three examples from the Utah temperature climatology we have stressed differences with MSIS90 or with what has been seen elsewhere. What is the origin of these differences? Did they arise because of differences in data-reduction algorithms or sample sizes? More interestingly, did they arise because of geographic location and differences in the orographic generation of gravity waves or because of time-varying phenomena like planetary waves with the concomitant generation of gravity waves by the jet stream? Of course, we believe the latter, but we need to prove it. Similarly, as more lidar facilities come on line, providing the world with more high-precision pinpoint measurements, such questions will continue to arise. How do we deal with them? It would be very useful to create a Lidar Working Group under which we could come together to sort them out. In comparing data, it would also be helpful to attempt to observe on many the same nights—for instance, during periods centered on the Incoherent Scatter Coordinated Observing Days on the International Geophysical Calendar. Such periods would be useful for obtaining simultaneous lidar data and for enabling us to contribute to a number of ongoing international programs, e.g., MLTCS—Mesosphere, Lower-Thermosphere Coupling Study.

References

1. Hedin, A.E.: Extension of the MSIS Thermosphere Model into the Middle and Lower Atmosphere, *J. Geophys. Res.* **96** (1991) 1159–1172.
2. Yu, J.R., She, C.Y.: Climatology of a Midlatitude Mesopause Region Observed by a Lidar at Fort Collins, Colorado (40.6°N, 105°W), *J. Geophys. Res.* **100** (1995) 7441–7452.
3. Hauchecorne, A., Chanin, M.L., Keckhut, P.: Climatology and Trends of the Middle Atmospheric Temperatures (33–87 km) as Seen by Rayleigh LIDAR over the South of France, *J. Geophys. Res.* **96** (1991) 15297–15309.
4. Clancy, R.T., Rusch, D.W., Callan, M.T.: Temperature Minima in the Average Thermal Structure of the Middle Mesosphere (70–80 km) from Analysis of 40- to 92-km SME Global Temperature Profiles, *J. Geophys. Res.* **99** (1994) 19001–19020.
5. Schmidlin, F.J.: Temperature Inversions near 75 km, *Geophys. Res. Lett.* **3** (1976) 173–176.
6. Hauchecorne, A., Chanin, M.L., Wilson, R.: Mesospheric Temperature Inversion and Gravity Wave Breaking, *Geophys. Res. Lett.* **14** (1987) 933–936.
7. Meriwether, J.W., Dao, P.D., McNutt, R.T., Klemetti, W., Moskowitz, W., Davidson, G.: Rayleigh Lidar Observations of Mesosphere Temperature Structure, *J. Geophys. Res.* **99** (1994) 16973–16987.
8. Whiteway, J.A., Carswell, A.I., Ward, W.E.: Mesospheric Temperature Inversions with Overlying Nearly Adiabatic Lapse Rate: an Indication of a Well-Mixed Turbulent Layer, *Geophys. Res. Lett.* **22** (1995) 1201–1204.